

Pauling Entropy, Metastability, and Equilibrium in $\text{Dy}_2\text{Ti}_2\text{O}_7$ Spin Ice

S. R. Giblin,^{1,*} M. Twengström,² L. Bovo,^{3,4} M. Ruminy,⁵ M. Bartkowiak,⁵ P. Manuel,⁶ J. C. Andresen,⁷ D. Prabhakaran,⁸ G. Balakrishnan,⁹ E. Pomjakushina,¹⁰ C. Paulsen,¹¹ E. Lhotel,¹¹ L. Keller,⁵ M. Frontzek,¹² S. C. Capelli,⁶ O. Zaharko,⁵ P. A. McClarty,¹³ S. T. Bramwell,³ P. Henelius,² and T. Fennell^{5,†}

¹*School of Physics and Astronomy, Cardiff University, Cardiff CF24 3AA, United Kingdom*

²*Department of Physics, Royal Institute of Technology, SE-106 91 Stockholm, Sweden*

³*London Centre for Nanotechnology and Department of Physics and Astronomy, University College London, 17-19 Gordon Street, London, WC1H 0AH, United Kingdom*

⁴*Department of Innovation and Enterprise, University College London,*

90 Tottenham Court Road, Fitzrovia, London W1T 4TJ, United Kingdom

⁵*Laboratory for Neutron Scattering and Imaging, Paul Scherrer Institut, CH-5232 Villigen PSI, Switzerland*

⁶*ISIS Facility, Rutherford Appleton Laboratory, Chilton, Didcot, OX11 0QX, United Kingdom*

⁷*Department of Physics, Ben Gurion University of the Negev, Beer Sheva 84105, Israel*

⁸*Clarendon Laboratory, Physics Department, Oxford University, Oxford, OX1 3PU, United Kingdom*

⁹*Department of Physics, University of Warwick, Coventry, CV4 7AL, United Kingdom*

¹⁰*Laboratory for Scientific Developments, Paul Scherrer Institut, CH-5232 Villigen PSI, Switzerland*

¹¹*Institut Néel, C.N.R.S—Université Joseph Fourier, B.P. 166, 38042 Grenoble, France*

¹²*Neutron Scattering Division, Oak Ridge National Laboratory, Oak Ridge, Tennessee, USA*

¹³*Max Planck Institute for the Physics of Complex Systems, Nöthnitzer Strasse 38, 01187 Dresden, Germany*



(Received 19 April 2018; published 7 August 2018)

Determining the fate of the Pauling entropy in the classical spin ice material $\text{Dy}_2\text{Ti}_2\text{O}_7$ with respect to the third law of thermodynamics has become an important test case for understanding the existence and stability of ice-rule states in general. The standard model of spin ice—the dipolar spin ice model—predicts an ordering transition at $T \approx 0.15$ K, but recent experiments by Pomaranski *et al.* suggest an entropy recovery over long timescales at temperatures as high as 0.5 K, much too high to be compatible with the theory. Using neutron scattering and specific heat measurements at low temperatures and with long timescales (0.35 K/ 10^6 s and 0.5 K/ 10^5 s, respectively) on several isotopically enriched samples, we find no evidence of a reduction of ice-rule correlations or spin entropy. High-resolution simulations of the neutron structure factor show that the spin correlations remain well described by the dipolar spin ice model at all temperatures. Furthermore, by careful consideration of hyperfine contributions, we conclude that the original entropy measurements of Ramirez *et al.* are, after all, essentially correct: The short-time relaxation method used in that study gives a reasonably accurate estimate of the equilibrium spin ice entropy due to a cancellation of contributions.

DOI: [10.1103/PhysRevLett.121.067202](https://doi.org/10.1103/PhysRevLett.121.067202)

The properties of ice-rule states, such as water ice [1,2] and spin ice [3–5], provide a strong contrast with the conventional paradigm of condensed matter. Instead of broken symmetry, entropy that vanishes in accord with the third law, exponentially decaying correlations, and wave-like excitations, one finds Coulomb phase correlations [6], finite entropy [1,5], and pointlike fractional excitations (monopoles) [7,8]. The mapping between the hydrogen bonding network and spin configurations [4,9] and the resultant identical residual (Pauling) entropy [5] are cornerstones of spin ice physics, posing fundamental questions including how a realistic Hamiltonian can lead to practical evasion of the third law, and whether the entropic state is metastable. Because the low-temperature dynamics of spin ice depends on a vanishing number of thermally excited monopoles, relaxation becomes slow at low temperatures

[2,10], and sensitivity to sample variations is enhanced [11,12]; both effects may mask the true equilibrium state. While the third law ground state of water ice can be accessed by doping that increases dynamics [9], the fate of the residual entropy in the spin ice $\text{Dy}_2\text{Ti}_2\text{O}_7$ [5] is unknown. Because of these experimental challenges, the problem of third law ordering in ice-type systems may best be addressed by a careful collaboration of experiment and theory, designed to accurately model the system and extrapolate properties beyond the experimental range.

The spin ice state of $\text{Dy}_2\text{Ti}_2\text{O}_7$ [3–5] is a consequence of frustration arising from the competition between the Ising-like crystal field anisotropy [13,14], exchange, and dipolar interactions [15,16]. These ingredients can be described by a classical spin Hamiltonian—the dipolar spin ice model (DSM) [15,16], which has been refined for many years

[17–19]. Theoretical investigations suggest that the dipolar spin ice states have a small bandwidth that eventually leads to an ordering transition and the recovery of the residual entropy [15–18]. However, several specific heat studies found no indication of ordering or reduction in the residual entropy, so the Hamiltonian parameters are required to suppress any such process below $T \sim 0.3$ K. Indeed, the population of monopole excitations becomes small below the freezing temperature, $T_f \approx 0.65$ K in $\text{Dy}_2\text{Ti}_2\text{O}_7$, where experimental timescales diverge exponentially. Recently, Pomaranski *et al.* [20] combined long equilibration times ($\approx 10^5$ s) with accurate temperature measurements to show that the specific heat apparently increases below 0.5 K. This experimental *tour de force* caused considerable excitement: Is the residual entropy recovered at a much higher temperature than predicted, indicating an insufficiency in the DSM that could allow an alternative, nonclassical ground state [19,21]?

Since performing equilibrated measurements much below T_f is challenging, a well-parametrized Hamiltonian model is important to allow for predictions of the low-temperature properties. Diffuse neutron scattering, a measure of the spin-spin correlation function, is well suited to directly test the Hamiltonian. However, the lowest temperature data used previously were obtained at 0.3 K with relatively short equilibration times ($\sim 10^3$ s) [22], a procedure that may be reasonably questioned [19] in light of the subsequently discovered long equilibration times. In this Letter, we describe neutron scattering measurements in the static approximation, designed to measure the spin and lattice temperatures of the sample, *in situ*. We verify the spin ice Hamiltonian with well-controlled equilibration at $T = 0.65$ K and, by monitoring the spin system *in situ* for $0.35 < T < 0.4$ K over a period $> 2 \times 10^6$ s, demonstrate that there is no evidence of any change in correlations or emergence of diffraction peaks in this temperature and time

window. Specific heat measurements on various isotopically enriched $\text{Dy}_2\text{Ti}_2\text{O}_7$ samples show that the system comes to thermodynamic equilibrium in this range, and we find no evidence for a recovery of the Pauling entropy at 0.5 K.

The sample studied using neutron scattering was the 1.4 g $^{162}\text{Dy}_2\text{Ti}_2\text{O}_7$ cuboid from Ref. [22]. For this work, the sample was reannealed in oxygen, and the SXD (ISIS, United Kingdom) [23] and TRiCS (PSI, Switzerland) [24] diffractometers used to confirm no structural diffuse scattering, indicative of oxygen defect clusters [12], was present [25]. Magnetic diffuse neutron scattering experiments were performed on the WISH (ISIS) [26] and DMC (PSI) [27] diffractometers (our procedures for data normalization for the two instruments are described in Ref. [25]). At DMC, Helmholtz coils reduced stray fields below $0.1 \mu\text{T}$. WISH has a stray field of $\approx 100 \mu\text{T}$. The crystal was clamped in a copper goniometer with a continuous thermal path to the mixing chamber (MC) of the dilution fridge. The clamp extends along 3/4 of the sample length, with a protruding few millimeters surrounded by an ac susceptometer that was thermalized by a deoxygenated copper braid to the MC end of the goniometer. The susceptometer was surrounded by neutron-absorbing cadmium. RuO_2 thermometers were attached to the goniometer (close to the sample) and the MC (12 cm apart). Because of the well-defined frequency dependence of the spin relaxation in $^{162}\text{Dy}_2\text{Ti}_2\text{O}_7$ [10,29,30], the susceptometer can measure the effective spin temperature, simultaneously with measurements of the lattice temperature by the sample thermometer. Figure 1(a) shows a representative relative susceptibility measurement, taken at 0.5 Hz, which shows a peak in the imaginary part centered around 0.64 K. From calibration measurements, it can be estimated that the coil set induces a small (0.02 K) heating effect, as the protruding part of the sample is not well thermally coupled, but the lattice and spin temperature are well coupled.

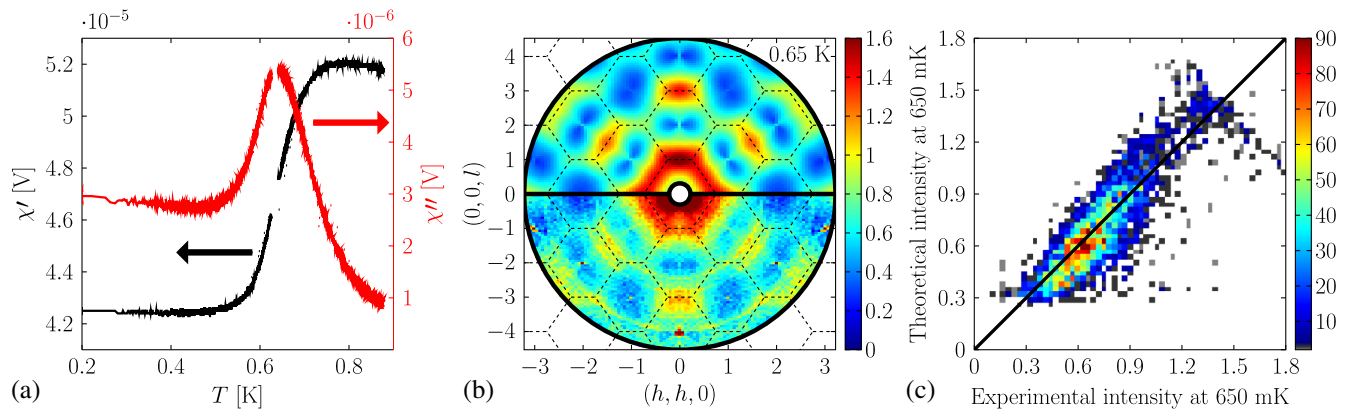


FIG. 1. Measurement of spin correlations with accurately equilibrated spin temperature of 0.65 K. (a) Example *in situ* susceptibility measurements (susceptibility χ is a linear function of the voltage). (b) The measured (lower hemisphere) and simulated (upper hemisphere) neutron structure factors are in close agreement. (c) Comparison of measured and calculated intensities (the color scale indicates the point density, with 11 518 points in total).

To model the neutron structure factor, we use the dipolar spin ice Hamiltonian

$$\mathcal{H} = \sum_{i>j} J_{ij} \mathbf{S}_i \cdot \mathbf{S}_j + Da^3 \sum_{i>j} \left(\frac{\mathbf{S}_i \cdot \mathbf{S}_j}{r_{ij}^3} - 3 \frac{(\mathbf{S}_i \cdot \mathbf{r}_{ij})(\mathbf{S}_j \cdot \mathbf{r}_{ij})}{r_{ij}^5} \right), \quad (1)$$

where \mathbf{S}_i are the spin vectors, a is the nearest neighbor distance, r_{ij} the distance separating particle i and j , D the dipolar constant [18], and J_{ij} a matrix describing the coupling strength between particles i and j . In this study, we used the g^+ -dipolar spin ice model (g^+ -DSM) parameters ($D = 1.3224$ K, $J_1 = 3.41$ K, $J_2 = -0.14$ K, $J_{3a} = 0.030$ K, and $J_{3b} = 0.031$ K) [25,28]. Using a parallel Monte Carlo code that exploits the symmetry of the dipolar interactions [31], we reached system sizes of $L = 16$ (65 536 spins), an order of magnitude larger and with improved resolution for $S(\mathbf{Q})$ than previous studies [19]. We used periodic Ewald boundary conditions [31] and a loop algorithm [16] to speed up equilibration. Using parallel tempering, we found the ordering temperature [16] of the g^+ DSM to be $T_c = 0.15$ K.

We verify that the g^+ -DSM parameters describe the neutron scattering data well at $T = 0.65$ K, the lowest temperature where we expect no equilibration issues (well below the existing data at 1.3 K [19]). At this temperature, the frequency dependence of the susceptibility allows the verification of the sample spin temperature and simultaneous measurement of the diffuse scattering (DMC). Figure 1(b) shows the experimental and simulated neutron structure factors for $T = 0.65$ K. The best fit of the theory to the experiment was made by scaling the experimental data, originally measured in “counts,” to the theoretical calculation using a linear function $S(\mathbf{Q})_{\text{theory}} = mS(\mathbf{Q})_{\text{experiment}} + c$ (where m is a scale parameter and c a

flat background contribution). m and c were determined through rms minimization in a region including the $(0,0,3)$ and $(3/2, 3/2, 3/2)$ peaks. As can be seen from the color map and the comparison of experimental and calculated intensities [Fig. 1(c)], the experimental and theoretical data match well at this temperature. The calculation captures the essence of the experimental data: the intensity and relative weight at $\mathbf{Q} = (0, 0, 3)$ and $\mathbf{Q} = (3/2, 3/2, 3/2)$ and the zone-boundary scattering, with no unexpected intensity at any wave vector. Similar agreement is obtained for $T = 1.3$ K [25]. We therefore expect that $\text{Dy}_2\text{Ti}_2\text{O}_7$ is well described by the g^+ DSM at a lower temperature, with an ordering transition around $T_c = 0.15$ K.

To examine lower-temperature equilibration and seek any behavior beyond the g^+ DSM, we needed to cool below T_f , ensuring we understood the thermal state of our sample during the measurements. Using a frequency of 0.5 Hz, we monitored the cooling of the sample for $0.5 \text{ K} < T < 0.9$ K. The lattice temperature and heat flows in or out of the sample can be monitored with the sample thermometer, and we saw that the spin temperature and lattice temperature were in equilibrium with each other and with the MC. There were identifiable sources of experimental heating below 0.5 K—by operating the susceptometer below 0.5 K, or below 0.3 K from the neutron beam. The neutron beam heating effect depends on the neutron flux and thermal coupling and so is experiment-specific. Measurements using the thermometer on the MC alone would not observe this heating, demonstrating the importance of *in situ* monitoring for poor thermal conductors.

We performed two experiments with different cooling protocols, producing identical results. We discuss the second, whose cooling protocol was longer than that of Pomaranski *et al.* [20,32]. Figure 2(a) shows the cooling of the thermometers attached to the goniometer and MC. These experiments were performed at WISH, cooling

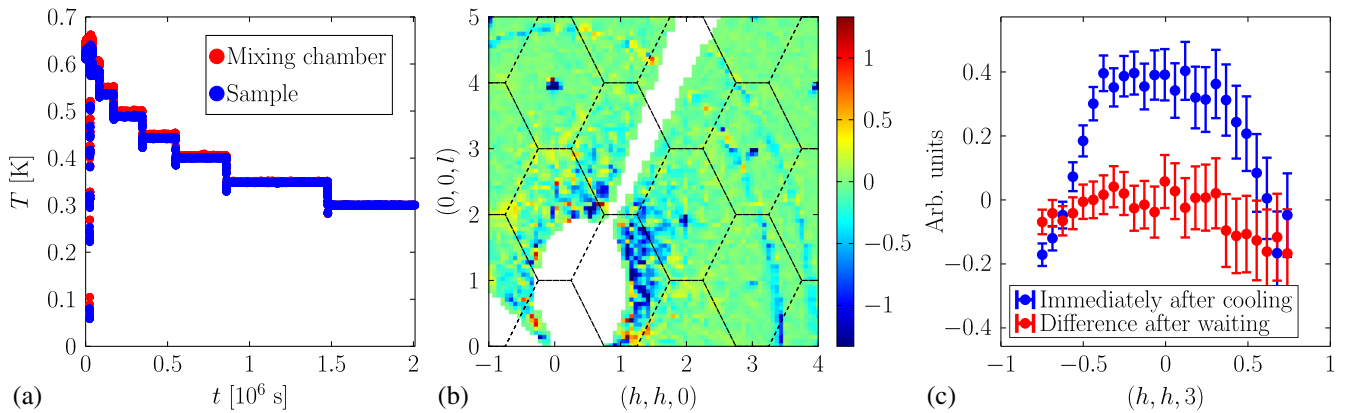


FIG. 2. Slow cooling and equilibration at 0.35 K. (a) The sample was cooled by a protocol similar to Ref. [20]. (b) Comparing a rapidly cooled measurement at 0.35 K with the slow-cooled measurement by taking the difference of the structure factors shows no difference between the two [data are normalized to match the scale of Fig. 1(b)]. (c) This is highlighted by comparing cuts across $(0,0,3)$ in the quenched and difference maps.

during an ISIS accelerator shutdown. To avoid self-heating effects, we made this measurement with the susceptometer switched off, having established that significant heat flows in and out of the sample can be recorded by the sample thermometer. The estimated equilibration time and beam heating constraints meant that our target temperature was 0.35 K. To investigate changes in the correlations with long equilibration times, we performed a difference measurement at 0.35 K. After standard cooling of the sample from 0.65 to 0.35 K (in some minutes), a map was recorded. We then warmed the sample to 0.65 K, followed the cooling protocol shown in Fig. 2(a), and recorded a second map at 0.35 K [25]. A difference map [Fig. 2(b)] shows no statistically significant difference between the normalized data [25], indicating that the previous low-temperature data, and analyses based on it [18,19,22], are trustworthy. A cut across $\mathbf{Q} = (0, 0, 3)$ for the difference of the two measurements is compared to the same cut for an unsubtracted data set in Fig. 2(c), again showing the absence of any feature in the difference. The g^+ -DSM parameters also reproduce this diffuse scattering well [25].

To seek further consistency, we performed specific heat measurements by the relaxation technique, paying particular attention to the long relaxation time [20] and the nuclear hyperfine interaction [19]. We used a Quantum Design PPMS with a ^3He insert, modified to allow relaxation times from 10^1 to 10^5 s, largely covering the timescales probed in Ref. [20]. We used three isotopes: an off cut of the $^{162}\text{Dy}_2\text{Ti}_2\text{O}_7$ neutron sample, with no nuclear spin ($I = 0$); an enriched $^{163}\text{Dy}_2\text{Ti}_2\text{O}_7$ sample with nuclear spin $I = 5/2$; and a sample with natural isotopic abundances $^{\text{Nat}}\text{Dy}$, containing ^{161}Dy and ^{163}Dy , both with nuclear spin $I = 5/2$, fractions 0.19 and 0.249, respectively, and the remainder with $I = 0$. The hyperfine energy is sufficiently small that the hyperfine specific heat C_H may be taken as equal to its high-temperature value $C_H = a/T^2$, where $a = 0, 0.026, 0.076 \text{ J K}^{-2} \text{ mol}^{-1}_{\text{Dy}}$ for ^{162}Dy , $^{\text{Nat}}\text{Dy}$, and

^{163}Dy , respectively [here $a = R(1/3)I(I+1)\epsilon^2$, ϵ is the effective energy separation of hyperfine levels, and R is the gas constant]. Adjusting for the incorrect nuclear spin (hyperfine) specific heat in Ref. [20] does not account for all the upturn in the specific heat [19] [see also Fig. 3(c)].

Figure 3(a) shows the specific heat of the three samples for two extreme relaxation times (12 and 89×10^4 s). A comparison of time-dependent measurements at the base temperature of 0.48 K (not shown) suggests that all samples reach complete thermodynamic equilibrium at $t \sim 10^5$ s, as found in Ref. [20]. Increasing the timescale leads to an increase in the specific heat, as found in Ref. [20]. Furthermore, the nuclear contribution is clearly visible at a low temperature: ^{162}Dy ($I = 0$) has the lowest specific heat and ^{163}Dy ($I = 5/2$) the highest.

Figure 3(b) shows the difference between the long- and short-time measurements for each sample, along with the hyperfine contribution for $^{\text{Nat}}\text{Dy}$. The short-time measurements remain in equilibrium to a lower temperature when there are more nuclear spins present. This indicates that the hyperfine energy levels provide additional relaxation paths for the electronic spins and also that the nuclear relaxation rate is on the same order as the electronic relaxation rate for $T \geq 0.55$ K.

Finally, we show the equilibrium electronic specific heat for the three samples, after the nuclear contribution has been subtracted in Fig. 3(c). Our main result is the comparison of the $^{\text{Nat}}\text{Dy}$ and the ^{162}Dy sample. Here, the subtraction of the hyperfine contribution projects the two curves accurately onto each other at all temperatures, revealing the equilibrium electronic specific heat (plus a negligible phonon contribution). We have high confidence in this result: The ^{162}Dy sample was removed from the larger sample that has been extensively characterized by neutron scattering, while the standard methods used to prepare the $^{\text{Nat}}\text{Dy}$ should render it relatively free of defects and impurities, as our results imply. In addition, the specific

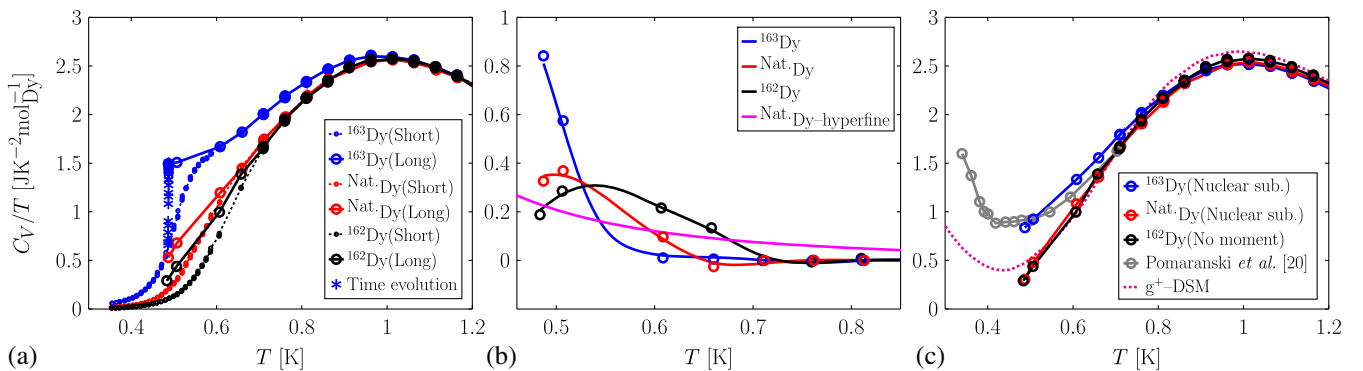


FIG. 3. Specific heat of ^{162}Dy , $^{\text{Nat}}\text{Dy}$, and ^{163}Dy samples of $\text{Dy}_2\text{Ti}_2\text{O}_7$. (a) Long- and short-time measurements. (b) Difference between long- and short-time measurements and calculated nuclear specific heat for the $^{\text{Nat}}\text{Dy}$ sample. (c) Equilibrium electronic specific heat for all samples, as well as model calculation and previous results from Ref. [20] (adjusted for the correct hyperfine contribution [19]). In (b) and (c), the lowest temperature displayed, 0.48 K, is the low-temperature limit of our long-time measurements.

heat of all three individual crystals, from two different crystal growers, collapse above 0.8 K, which is not the case for many previous measurements [20]. This experimental equilibrium curve is well, but not perfectly, matched by the g^+ DSM. These slight discrepancies are due to the fact that the original g -DSM parameters [18] were adjusted to short-time specific heat data that were slightly higher [33]. Further fine-tuning of the parameters is possible but beyond this study. Our experiments establish that there is no upturn in the equilibrated electronic specific heat above $T = 0.5$ K, a conclusion fully consistent with the theory and our neutron measurements.

Our results suggest that the most likely cause for the upturn observed by Pomaranski *et al.* [20] is random disorder, in agreement with Ref. [19]. Magnetic defects introduce localized energy levels, which will increase the specific heat per magnetic ion, so spin ice samples with the largest equilibrium (or long-time) specific heat tend to be the most defective, as our study implies. Our work suggests that a careful study correlating the consequences of different types of defects (e.g., oxygen deficiency [12] or “stuffing” [11,34]) in structural and magnetic measurements, as has been done for $\text{Yb}_2\text{Ti}_2\text{O}_7$ [35] and $\text{Tb}_2\text{Ti}_2\text{O}_7$ [36], would be of considerable value.

Reconsidering now the short-time measurements in Fig. 3(a), we note that the short-time curve for the ^{163}Dy sample is not so far away from the final equilibrium curve, the long-time curve for the ^{162}Dy sample. Hence, the uncorrected short-time results of Ramirez *et al.* [5] and other authors are reasonable estimates of the equilibrium electronic specific heat. The reason for this is a cancellation of terms: Adding the long-time contribution and subtracting the nuclear part leads to only a small net change in the specific heat, since these terms are roughly equal; see Fig. 3(b). Also notable is that the short-time measurements of all three samples converge below 0.4 K. This suggests that the nuclear relaxation time becomes much greater than the electronic one at a low temperature and that the hyperfine specific heat is not visible in a short-time measurement for $T \leq 0.45$ K [37].

In conclusion, this Letter addresses a specific case of the more general question: How can we know the third law ground state of ice-type systems, whose dynamics depend on a vanishing number of pointlike excitations (monopoles)? When the monopole density becomes small, extrinsic defects and disorder become important: In the case of water ice, they are thought to provide sufficient dynamics to locate the ground state [9], but there seems to be no comparable mechanism available in spin ice. In $^{162}\text{Dy}_2\text{Ti}_2\text{O}_7$, we have carefully equilibrated the sample at 0.65 and 0.35 K, demonstrating the value of measuring the temperature of both the spin and lattice baths when characterizing such systems using neutron scattering. By confirming the accuracy of the dipolar spin ice model in this range, we support the “monopole fluid” picture of spin

ice [8] and the interesting theories and experiments that arise from it [11,38–40]. We predict the recovery of the Pauling entropy at lower temperatures, and our work highlights the experimental temperature and time windows that would have to be accessed to detect effects beyond the standard model of spin ice.

We thank Jan Kycia and David Pomaranski for sharing the cooling protocol of Ref. [20], Michel Gingras for useful discussions and suggestions, the late Shaun Fisher for a selection of calibrated thermometers, and the ISIS sample environment team. The simulations were performed on resources provided by the Swedish National Infrastructure for Computing (SNIC) at the Center for High Performance Computing (PDC) at the Royal Institute of Technology (KTH). M. T. and P. H. are supported by the Swedish Research Council (2013-03968), M. T. is grateful for funding from Stiftelsen Olle Engkvist Byggmästare (2014/807), M. R. was supported by the SNSF (Schweizerischer Nationalfonds zur Förderung der Wissenschaftlichen Forschung) (Grant No. 200021_140862), and L. B. was supported by The Leverhulme Trust through the Early Career Fellowship program (ECF2014-284). G. B. thanks EPSRC, United Kingdom for funding through Grant No. EP/M028771/1.

S. R. G., M. R., M. B., P. M., T. F., M. T., and P. A. M. performed neutron scattering experiments (with L. K. and M. F. at PSI). S. R. G., M. B., C. P., and E. L. designed, constructed, and calibrated the susceptometer and thermometry. M. T., S. R. G., M. R., and P. H. analyzed neutron scattering data and compared to simulations. M. R., E. P., T. F., S. R. G., P. M., O. Z., and S. C. C. reannealed and characterized the $^{162}\text{Dy}_2\text{Ti}_2\text{O}_7$ crystal. L. B., S. T. B., and P. H. developed and carried out the specific heat measurements and their analysis. M. T., J. C. A., and P. H. developed and carried out the Monte Carlo simulations. D. P. and G. B. grew the crystals (^{163}Dy and ^{162}Dy , respectively). S. R. G., M. T., S. T. B., P. H., and T. F. wrote the paper with input from all authors.

*giblinr@cardiff.ac.uk

†tom.fennell@psi.ch

- [1] L. Pauling, *J. Am. Chem. Soc.* **57**, 2680 (1935).
- [2] W. F. Giauque and J. W. Stout, *J. Am. Chem. Soc.* **58**, 1144 (1936).
- [3] M. J. Harris, S. T. Bramwell, D. F. McMorrow, T. Zeiske, and K. W. Godfrey, *Phys. Rev. Lett.* **79**, 2554 (1997).
- [4] S. T. Bramwell and M. J. Harris, *J. Phys. Condens. Matter* **10**, L215 (1998).
- [5] A. P. Ramirez, A. Hayashi, R. J. Cava, R. Siddharthan, and B. S. Shastry, *Nature (London)* **399**, 333 (1999).
- [6] T. Fennell, P. P. Deen, A. R. Wildes, K. Schmalzl, D. Prabhakaran, A. T. Boothroyd, R. J. Aldus, D. F. McMorrow, and S. T. Bramwell, *Science* **326**, 415 (2009).
- [7] I. A. Ryzhkin, *J. Exp. Theor. Phys.* **101**, 481 (2005).

- [8] C. Castelnovo, R. Moessner, and S. L. Sondhi, *Nature (London)* **451**, 42 (2008).
- [9] Y. Tajima, T. Matsuo, and H. Suga, *Nature (London)* **299**, 810 (1982).
- [10] J. Snyder, B. G. Ueland, J. S. Slusky, H. Karunadasa, R. J. Cava, and P. Schiffer, *Phys. Rev. B* **69**, 064414 (2004).
- [11] H. M. Revell, L. R. Yaraskavitch, J. D. Mason, K. A. Ross, H. M. L. Noad, H. A. Dabkowska, B. D. Gaulin, P. Henelius, and J. B. Kycia, *Nat. Phys.* **9**, 34 (2013).
- [12] G. Sala, M. J. Gutmann, D. Prabhakaran, D. Pomaranski, C. Michelitis, J. B. Kycia, D. G. Porter, C. Castelnovo, and J. P. Goff, *Nat. Mater.* **13**, 488 (2014).
- [13] A. Bertin, Y. Chapuis, P. D. de Réotier, and A. Yaouanc, *J. Phys. Condens. Matter* **24**, 256003 (2012).
- [14] M. Ruminy, E. Pomjakushina, K. Iida, K. Kamazawa, D. T. Adroja, U. Stuhr, and T. Fennell, *Phys. Rev. B* **94**, 024430 (2016).
- [15] B. C. den Hertog and M. J. P. Gingras, *Phys. Rev. Lett.* **84**, 3430 (2000).
- [16] R. G. Melko, B. C. den Hertog, and M. J. P. Gingras, *Phys. Rev. Lett.* **87**, 067203 (2001).
- [17] J. P. C. Ruff, R. G. Melko, and M. J. P. Gingras, *Phys. Rev. Lett.* **95**, 097202 (2005).
- [18] T. Yavors'kii, T. Fennell, M. J. P. Gingras, and S. T. Bramwell, *Phys. Rev. Lett.* **101**, 037204 (2008).
- [19] P. Henelius, T. Lin, M. Enjalran, Z. Hao, J. G. Rau, J. Altsaar, F. Flicker, T. Yavors'kii, and M. J. P. Gingras, *Phys. Rev. B* **93**, 024402 (2016).
- [20] D. Pomaranski, L. R. Yaraskavitch, S. Meng, K. A. Ross, H. M. L. Noad, H. A. Dabkowska, B. D. Gaulin, and J. B. Kycia, *Nat. Phys.* **9**, 353 (2013).
- [21] P. A. McClarty, O. Sikora, R. Moessner, K. Penc, F. Pollmann, and N. Shannon, *Phys. Rev. B* **92**, 094418 (2015).
- [22] T. Fennell, O. A. Petrenko, B. Fåk, S. T. Bramwell, M. Enjalran, T. Yavors'kii, M. J. P. Gingras, R. G. Melko, and G. Balakrishnan, *Phys. Rev. B* **70**, 134408 (2004).
- [23] D. A. Keen, M. J. Gutmann, and C. C. Wilson, *J. Appl. Crystallogr.* **39**, 714 (2006).
- [24] J. Schefer, M. Könnecke, A. Murasik, A. Czopnik, T. Strässle, P. Keller, and N. Schlumpf, *Physica (Amsterdam) B* **276–278**, 168 (2000).
- [25] See Supplemental Material at <http://link.aps.org/supplemental/10.1103/PhysRevLett.121.067202> for experimental and computational details [12,18,23,26–28].
- [26] L. C. Chapon, P. Manuel, P. G. Radaelli, C. Benson, L. Perrott, S. Ansell, N. J. Rhodes, D. Raspino, D. Duxbury, E. Spill, and J. Norris, *Neutron News* **22**, 22 (2011).
- [27] J. Schefer, P. Fischer, H. Heer, A. Isacson, M. Koch, and R. Thut, *Nucl. Instrum. Methods Phys. Res., Sect. A* **288**, 477 (1990).
- [28] L. Bovo, M. Twengström, O. A. Petrenko, T. Fennell, M. J. P. Gingras, S. T. Bramwell, and P. Henelius, *Nat. Commun.* **9**, 1999 (2018).
- [29] K. Matsuhira, C. Paulsen, E. Lhotel, C. Sekine, Z. Hiroi, and S. Takagi, *J. Phys. Soc. Jpn.* **80**, 123711 (2011).
- [30] L. R. Yaraskavitch, H. M. Revell, S. Meng, K. A. Ross, H. M. L. Noad, H. A. Dabkowska, B. D. Gaulin, and J. B. Kycia, *Phys. Rev. B* **85**, 020410 (2012).
- [31] P. P. Ewald, *Ann. Phys. (Berlin)* **369**, 253 (1921).
- [32] J. B. Kycia (private communication).
- [33] R. Higashinaka, H. Fukazawa, and Y. Maeno, *Phys. Rev. B* **68**, 014415 (2003).
- [34] G. C. Lau, R. S. Freitas, B. G. Ueland, B. D. Muegge, E. L. Duncan, P. Schiffer, and R. J. Cava, *Nat. Phys.* **2**, 249 (2006).
- [35] K. A. Ross, T. Proffen, H. A. Dabkowska, J. A. Quilliam, L. R. Yaraskavitch, J. B. Kycia, and B. D. Gaulin, *Phys. Rev. B* **86**, 174424 (2012).
- [36] T. Taniguchi, H. Kadowaki, H. Takatsu, B. Fak, J. Ollivier, T. Yamazaki, T. J. Sato, H. Yoshizawa, Y. Shimura, T. Sakakibara, T. Hong, K. Goto, L. R. Yaraskavitch, and J. B. Kycia, *Phys. Rev. B* **87**, 060408 (2013).
- [37] E. Bertin, P. Bonville, J.-P. Bouchaud, J. Hodges, J. Sanchez, and P. Vulliet, *Eur. Phys. J. B* **27**, 347 (2002).
- [38] C. Paulsen, S. R. Giblin, E. Lhotel, D. Prabhakaran, G. Balakrishnan, K. Matsuhira, and S. T. Bramwell, *Nat. Phys.* **12**, 661 (2016).
- [39] V. Kaiser, S. T. Bramwell, P. C. W. Holdsworth, and R. Moessner, *Phys. Rev. Lett.* **115**, 037201 (2015).
- [40] V. Kaiser, J. Bloxsom, L. Bovo, S. T. Bramwell, P. C. W. Holdsworth, and R. Moessner, arXiv:1803.04668.